Zemin Mekaniği ve Geoteknik Mühendisliği
20. Ulusal Konferansı

15-16 Ekim 2026
Sakarya Üniversitesi

PLASTİK OLMAYAN İNCE DANELERİN ZEMİNLERİN ÇEVRİMSEL DAYANIMI ÜZERİNDEKİ ETKİLERİ

EFFECTS OF NON-PLASTIC FINES ON CYCLIC RESISTANCE OF SOILS

Atasev Dogukan TASBASI[1], Kemal Onder CETIN[2], Moutasem ZARZOUR[3], Ahmed AL-SUHAILY[4], Eylem ARSLAN[5], Kadir KOCAMAN[6], Ertan BOL[7], Aşkın OZOCAK[8], Sedat SERT[9]

ÖZET

Bu çalışma, plastik olmayan ince tanelerin zeminlerin çevrimsel dayanımı üzerindeki etkilerini, temiz kumlar ile plastik olmayan siltlerin davranışını karşılaştırarak incelemektedir. Sabit hacimli çevrimsel doğrudan basit kesme (CDSS) deneylerinden elde edilen kapsamlı bir deneysel veri tabanı kullanılmıştır. Temiz kum davranışı yeniden oluşturulmuş Çine kumu numuneleri ile temsil edilirken, plastik olmayan silt davranışı ihmal edilebilir kil içeriğine sahip yeniden oluşturulmuş Adapazarı silt numuneleri ile karakterize edilmiştir. Numuneler hava ile serbest serme yöntemi kullanılarak hazırlanmış ve 50, 100 ve 200 kPa başlangıç düşey efektif gerilmeler altında deneylere tabi tutulmuştur. Daha sonra numunelere, sabit 3 mm/dk kesme deformasyon hızı altında tek yönlü çevrimsel kesme gerilmeleri uygulanmış ve deneyler, maksimum çevrimsel kesme deformasyonu veya r_u değerinin sırasıyla yaklaşık %30 ya da 1'e ulaşmasına kadar sürdürülmüştür. Her iki malzemenin çevrimsel dayanımı, çevrimsel gerilme oranı (CSR) ve %5 çift genlikli kesme şekil değiştirmesine ulaşmak için gereken çevrim sayısı cinsinden değerlendirilmiştir. Bu çalışmada, temiz kum ve plastik olmayan siltlerin çevrimsel davranışları karşılaştırılarak aralarındaki farklar ortaya konmuştur. Deney sonuçları $CSR - N$ düzleminde sunulmuş ve farklı başlangıç düşey efektif gerilme ($\sigma'_{v,0}$), konsolidasyon sonrası boşluk oranı (e_c) ve γ_{DA} değerleri için dayanım eğrileri geliştirilmiştir.

Anahtar Kelimeler: *Sıvılaşma, Doğrudan Basit Kesme Deneyi, Tek Yönlü Çevrimsel Yükleme, Saf Adapazarı Siltleri, Çine Kumu*

ABSTRACT

This study investigates the effects of non-plastic fines on the cyclic resistance of soils by comparing the behavior of clean sands and non-plastic silts. A comprehensive experimental database obtained from constant-volume cyclic direct simple shear (CDSS) tests is utilized. The clean sand behavior is represented by reconstituted Çine sand samples, while the non-plastic silt behavior is characterized using reconstituted Adapazarı silt samples with negligible clay content. The specimens were prepared using air pluviation method and tested under initial vertical effective stresses of 50, 100 and 200 kPa. They were then subjected to unilateral cyclic shear stresses at a constant shear strain rate of 3 mm/min until a peak cyclic shear strain or

[1] Arş. Gör., Orta Doğu Teknik Üniversitesi, atasevt@metu.edu.tr (Sorumlu yazar)
[2] Prof. Dr., Orta Doğu Teknik Üniversitesi, kemalondercetin@gmail.com
[3] Dr., Orta Doğu Teknik Üniversitesi, eng.moutasemz@gmail.com
[4] Dr., ALFA Testing Equipment, ahmed_suhaily@yahoo.com
[5] Arş. Gör., Sakarya Üniversitesi, eylemarslan@sakarya.edu.tr
[6] Arş. Gör., Sakarya Üniversitesi, kadirkocaman@sakarya.edu.tr
[7] Prof. Dr., Sakarya Üniversitesi, ebol@sakarya.edu.tr
[8] Prof. Dr., Sakarya Üniversitesi, aozocak@sakarya.edu.tr
[9] Prof. Dr., Sakarya Üniversitesi, sert@sakarya.edu.tr

the r_u values reached about of 30% or 1, respectively. The cyclic resistance of both materials is evaluated in terms of cyclic stress ratio (CSR) and number of cycles to reach a double amplitude shear strain level of 5%. In this study, a comparative assessment is performed to highlight the differences in cyclic response between clean sand and non-plastic silts. Test results were presented in the $CSR - N$ domain, with resistance curves developed for varying ($\sigma'_{v,0}$), post-consolidation void ratios (e_c), and γ_{DA} values.
Keywords: *Liquefaction, Direct Simple Shear Test, Unidirectional Cyclic Loading, Pure Adapazarı Silts, Çine Sand*

1. INTRODUCTION

The accurate evaluation of soil liquefaction and cyclic softening behavior under seismic loading remains one of the most critical and evolving areas of geotechnical earthquake engineering. Past earthquake case histories, such as the 1999 Kocaeli earthquake (M_w = 7.5) in Türkiye, demonstrated that silt-rich deposits in the Adapazarı-Sakarya region suffered severe ground distresses, ground failures, and large permanent soil deformations, even under relatively low peak ground surface accelerations (Cetin et al., 2004). While the cyclic behavior of clean sands has been extensively studied in the literature and incorporated into simplified liquefaction triggering assessment frameworks, the geotechnical behavior of non-plastic silts is less understood due to their transitional nature between cohesionless sands and cohesive clays (Ishihara, 1993).

In engineering practice, when analyzing the liquefaction resistance of soils, the effect of fines content (FC) is often evaluated independently of the plasticity index (PI) or is limited to standard empirical corrections. However, the skeleton structure, particle size, and grain contact mechanisms of non-plastic silty soils differ significantly from those of clean sands. These differences directly influence the cyclic shear resistance developed at the same skeletal relative density or effective confining stress state (Boulanger, 2003). Therefore, isolating the role of non-plastic fines on the cyclic resistance of soils at an experimental level through controlled laboratory testing and directly comparing it with clean sand behavior is of paramount importance.

The primary objective of this study is to investigate the effects of non-plastic fines on soil strength by comparing the behavior of clean sands and non-plastic silts. For this purpose, reconstituted Çine sand samples representing clean sand behavior and reconstituted pure Adapazarı silt samples with negligible clay content characterizing non-plastic silt behavior were used. The tests were performed using a multi-directional cyclic direct simple shear (CDSS) apparatus developed under the supervision of the second author. The experimental database obtained for both soil types under different void ratios, relative densities, and confining stress conditions was compared based on skeleton void ratio and structural fabric relationships. In this manner, the effect of non-plastic fines content on strength mechanisms was isolated without cohesive or plastic influences.

2. MATERIAL PROPERTIES AND TEST SET-UP

2.1. Material Characterization

The Çine sand used in this study is mineralogically composed mostly of quartz, classified as poorly graded fine sand (SP) with a uniformity coefficient (c_u) of 3.48 and a coefficient of curvature (c_c) of 1.02 (Al-Suhaily, 2025). The specific gravity (G_s) of Çine sand is 2.660, with a maximum void ratio (e_{max}) of 0.825 and a minimum void ratio (e_{min}) of 0.505. From a particle geometry perspective, its sphericity is 0.58 and its roundness is 0.28, determined according to the method proposed by Aksoy (2024).

The comparison material, Adapazarı silt, was obtained from floodplain deposits along the banks of the Sakarya River, indicating a fluvial origin (Bol, 2003). To preserve its pure silt character and prevent clay content from inducing plastic effects, the clay fraction was reduced to less than 5% using a flotation/sedimentation technique. The resulting tested soil consists of over 95% silt-size particles and is classified as completely non-plastic silt (ML) based on the USCS. The specific gravity of Adapazarı silt is 2.653, with a minimum void ratio of 0.895 and a maximum void ratio of 1.411. All physical and index properties of both materials are summarized comparatively in Table 1.

Table 1. Index properties of Çine sand and Adapazarı silt

Index Property / Parameter	Çine Sand	Adapazarı Silt	Method / Notes
USCS Classification	SP	ML	ASTM D2487
Clay Content (< 2 µm, %)	0.0%	< 5.0%	ASTM D7928 (Sedimentation)
Silt Content (2–75 µm, %)	1.35%	> 95.0%	ASTM D1140 (Wet Sieving)
Sand Content (> 75 µm, %)	98.65%	~ 0.0%	ASTM D6913 (Dry Sieving)
Plasticity Index (PI, %)	NP (Non-plastic)	NP (Non-plastic)	ASTM D4318
Maximum Void Ratio (e_{max})	0.825	1.411	ASTM D4254 (Modified)
Minimum Void Ratio (e_{min})	0.505	0.895	ASTM D4253 (Modified)
Specific Gravity (G_s)	2.660	2.653	ASTM D854
Particle Roundness (R)	0.28	-	Aksoy (2024)
Particle Sphericity (S)	0.58	-	Aksoy (2024)

2.2. Sample Preparation Methods

Reconstituting soil samples in the laboratory with repeatable initial fabric and particle arrangements is highly critical for the reliability of shear strength results. Dry Çine sand specimens were prepared using the funnel deposition method (Al-Suhaily, 2025). Prior to consolidation, the samples were placed at target void ratios corresponding to loose (25%), medium (41.6%), and dense (80%) relative densities. The setup of the sand samples in the CDSS device was carried out using a low-friction stacked shear-ring lateral confinement system and a thin latex membrane to restrict lateral deformations.

Conversely, dry Adapazarı silt specimens were prepared using the air pluviation method to achieve a uniform fabric and homogeneous vertical particle deposition (Tasbasi et al., 2025). By adjusting the pluviation height and drop rate, loose (27.9%), medium (43.8%), and dense (77.1%) initial relative density states were achieved. To standardize the silt samples, repeatability was ensured using a custom-made, 3D-printed height referencing ring and a specialized tamper, which can be seen in Figure 1.

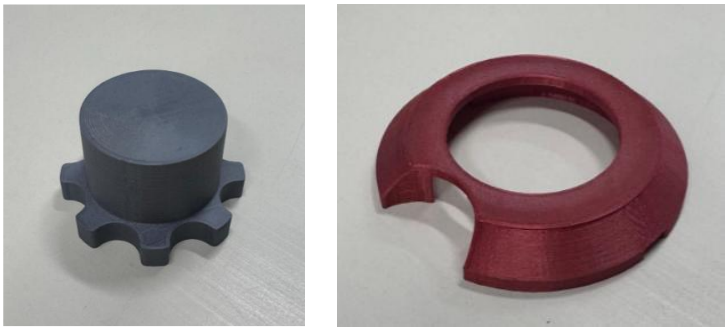

(a) (b)

Figure 1. (a) 3D printed tamper (b) height referencing ring (Tasbasi et al., 2025)

2.3. Multidirectional Cyclic Direct Simple Shear Device

Cyclic shear tests were performed using a multidirectional cyclic direct simple shear test set-up, which is capable of applying stress- or strain-controlled dynamic loads vertically and in two orthogonal horizontal directions. CDSS tests were conducted under constant-volume conditions. Vertical deformations in the specimen, which is confined by low-friction metal shear-rings, are prevented by a closed-loop control system. Since volumetric change is prevented, the observed decrease in vertical effective stress is considered directly equivalent to the undrained excess pore pressure ratio (r_u) generated during an earthquake (Ishihara, 1993).

During the tests, data logging was performed using a 24-bit FastDAQ data acquisition system recording at a rate of 80 samples per second. To prevent loading frequency from inducing equipment resonance in soft silts and clays and to simulate realistic seismic shear strain rates, the tests were conducted at specified shear displacement rates. In this study, a constant shearing velocity of 3 mm/min (0.05 mm/s) was selected for the Adapazarı silt tests. The Çine sand tests were also conducted at the same shear strain rate under unidirectional cyclic loading. The specimens were initially consolidated to vertical effective stresses of 50, 100, and 200 kPa under K_0 conditions, and subsequently subjected to cyclic shearing at varying Cyclic Stress Ratios (CSR).

3. RESULTS AND ANALYSIS

Adapazarı silt and Çine sand specimens were prepared at three different relative densities to represent loose, medium, and dense states. Prior to the consolidation stage, target relative densities of 27.9%, 43.8%, and 77.1% were achieved for the loose, medium, and dense conditions, respectively for the Adapazarı silt specimens. On the other hand, loose, medium and dense conditions were represented by relative densities of 25%, 41.6% and 80%, respectively for the Çine sand specimens. These density states were selected to systematically investigate and compare the influence of initial packing on the cyclic response of the silts and sands under varying confining stresses. To establish a controlled testing environment, the silt and sand specimens were exposed to a constant set of consolidation stresses of 50, 100 and 200 kPa for each of these relative density levels. The testing was stopped when the double amplitude shear strain reached a threshold of around 30%, or the r_u value reached about 1. Details of the cyclic tests can be seen in Table 2.

Table 2. Cyclic test details

Test ID	Test Type	Constant Strain Rate (mm/min)	Consolidation Stress, $\sigma'_{v,0}$ (kPa)	CSR	Pre-consolidation Relative Density, D_R (%)	Initial Void Ratio (e_0)	Preshear Void Ratio (e_C)
ADAP-01	Cyclic	3	50	0.110	27.9	1.267	0.759
ADAP-02				0.125		1.264	0.666
ADAP-03				0.145		1.267	0.764
ADAP-04				0.135	43.8	1.185	0.685
ADAP-05				0.155		1.185	0.831
ADAP-06				0.175	77.1	1.013	0.760
ADAP-07			100	0.110	27.9	1.268	1.218
ADAP-08				0.120		1.267	1.217
ADAP-09				0.140		1.267	1.214
ADAP-10				0.130	43.8	1.185	1.135
ADAP-11				0.100		1.190	1.146

Test ID	Test Type	Constant Strain Rate (mm/min)	Consolidation Stress, $\sigma'_{v,0}$ (kPa)	CSR	Pre-consolidation Relative Density, D_R (%)	Initial Void Ratio (e_0)	Preshear Void Ratio (e_C)
ADAP-12	Cyclic	3	100	0.110	43.8	1.185	1.139
ADAP-13				0.170		1.013	0.978
ADAP-14				0.140	77.1	1.016	0.983
ADAP-15				0.125		1.011	0.977
ADAP-16			200	0.141		1.265	0.716
ADAP-17				0.120	27.9	1.267	0.735
ADAP-18				0.135		1.271	1.041
ADAP-19				0.110		1.188	0.893
ADAP-20				0.125	43.8	1.185	0.809
ADAP-21				0.145		1.184	0.950
ADAP-22				0.155		1.015	0.616
ADAP-23				0.190	77.1	1.012	0.608
ADAP-24				0.165		1.011	0.600
S-1			50	0.144		0.745	0.724
S-2				0.104	25	0.745	0.722
S-3				0.124		0.745	0.719
S-4				0.093		0.745	0.718
S-5				0.100		0.692	0.668
S-6				0.148		0.692	0.674
S-7				0.122	41.6	0.692	0.672
S-8				0.162		0.692	0.672
S-9				0.112		0.692	0.673
S-10				0.147		0.569	0.554
S-11				0.193		0.569	0.552
S-12				0.117	80	0.569	0.540
S-13				0.135		0.569	0.541
S-14				0.096		0.569	0.547
S-15				0.235		0.569	0.553
S-16			100	0.100		0.745	0.650
S-17				0.146		0.745	0.662
S-18				0.125		0.745	0.659
S-19				0.131	25	0.745	0.707
S-20				0.135		0.745	0.713
S-21				0.082		0.745	0.713
S-22				0.103		0.745	0.710
S-23				0.100		0.692	0.662
S-24				0.204		0.692	0.660
S-25				0.141		0.692	0.663
S-26				0.102	41.6	0.692	0.666
S-27				0.122		0.692	0.667
S-28				0.120		0.692	0.667
S-29				0.119		0.692	0.661
S-30				0.197		0.569	0.545
S-31				0.100		0.569	0.543
S-32				0.197	80	0.569	0.545
S-33				0.152		0.569	0.542
S-34				0.109		0.569	0.544
S-35				0.121		0.569	0.545
S-36			200	0.152		0.745	0.660
S-37				0.100	25	0.745	0.657
S-38				0.126		0.745	0.660
S-39				0.080		0.745	0.688

Test ID	Test Type	Constant Strain Rate (mm/min)	Consolidation Stress, $\sigma'_{v,0}$ (kPa)	CSR	Pre-consolidation Relative Density, D_R (%)	Initial Void Ratio (e_0)	Preshear Void Ratio (e_C)
S-40	Cyclic	3	200	0.201	41.6	0.692	0.666
S-41				0.140		0.692	0.653
S-42				0.121		0.692	0.659
S-43				0.150		0.692	0.665
S-44				0.101		0.692	0.657
S-45				0.172		0.692	0.662
S-46				0.101		0.692	0.657
S-47				0.124		0.692	0.657
S-48				0.101		0.692	0.653
S-49				0.302	80	0.569	0.544
S-50				0.255		0.569	0.547
S-51				0.201		0.569	0.545
S-52				0.102		0.569	0.545
S-53				0.159		0.569	0.554
S-54				0.120		0.569	0.540
S-55				0.159		0.569	0.536

To evaluate and compare the cyclic resistance of clean Çine sand and non-plastic Adapazarı silt, test results were plotted in the $CSR - N_{\gamma DA=5\%}$ space ($N_{\gamma DA=5\%}$ representing the number of cycles to reach a double amplitude shear strain level of γ_{DA} = 5%). The comparative analysis is structured into three primary subsections based on the target density states: loose ($D_r \approx$ 25% - 27.9%), medium dense ($D_r \approx$ 41.6% - 43.8%), and dense $D_r \approx$ 77.1% - 80%) conditions. Within each density condition, the response under initial vertical effective stresses of 50, 100, and 200 kPa is examined sequentially.

3.1. Cyclic Resistance at Loose State

At loose states, both materials exhibit a highly contractive soil skeleton under cyclic simple shear loading. For all applied initial vertical effective stresses, the $CSR - N_{\gamma DA=5\%}$ strength curves of Çine sand and Adapazarı silt show a striking overlap. Even though clean sands are conventionally anticipated to offer higher cyclic resistance than fine-grained soils, the extremely loose arrangement of Çine sand leads to rapid mechanical stress degradation and swift shear strain accumulation. On the other hand, the non-plastic Adapazarı silt demonstrates a virtually identical cyclic resistance trend. The comparative $CSR - N_{\gamma DA=5\%}$ relationships at loose state for initial vertical effective stress levels of 50, 100, and 200 kPa are presented in Figure 2a, 2b, and 2c, respectively.

The slight density advantage of the silt ($\Delta D_r \approx$ +3%) compensates for the absence of a pure sand skeleton. Consequently, under low relative density conditions, non-plastic silt matrix behavior mimics clean loose sand, yielding superposed $CSR - N$ failure envelopes across all tested confining stress levels.

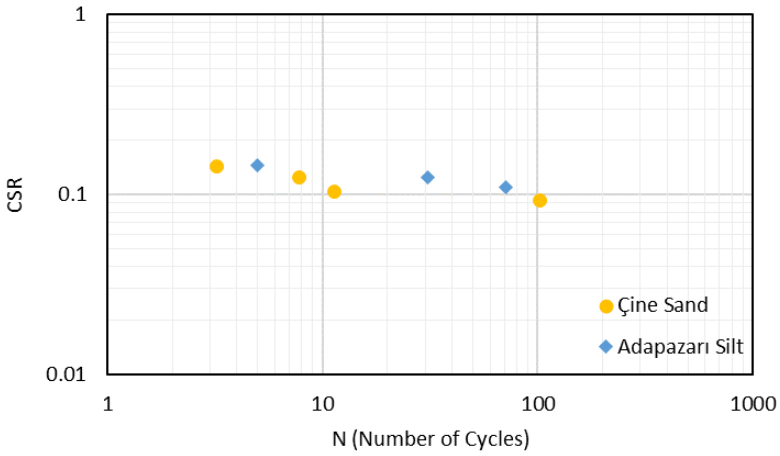

(a) $\sigma'_{v,0}$ = 50 kPa

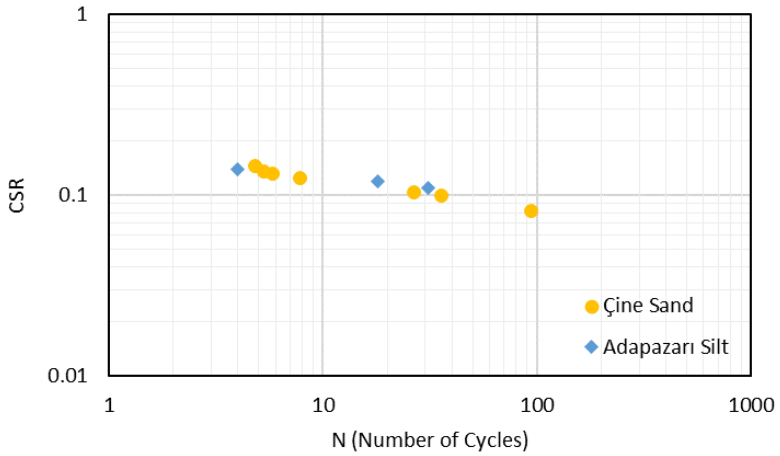

(b) $\sigma'_{v,0}$ = 100 kPa

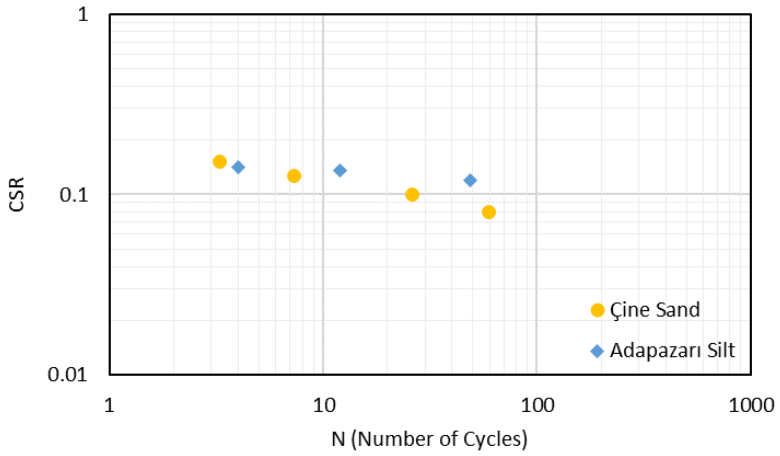

(c) $\sigma'_{v,0}$ = 200 kPa

Figure 2. Comparison of cyclic resistance curves for loose Çine sand and Adapazarı silt under initial vertical effective stress states of: (a) 50 kPa, (b) 100 kPa, and (c) 200 kPa

3.2. Cyclic Resistance at Medium Dense State

At medium dense initial states, the cyclic shear response reflects a transitional behavior between purely contractive volume loss tendency and dilatant strain hardening. Comparing the $CSR - N_{\gamma DA=5\%}$ trends at these vertical effective stresses reveals that non-plastic Adapazarı silt maintains a cyclic resistance capacity comparable to clean Çine sand. In this density range, fine silt particles fill the intergranular void space without inducing cohesive plasticity, thereby stabilizing the grain contact skeleton under constant-volume shearing. As a result, the rate of cyclic strain accumulation and vertical effective stress loss in pure silt aligns closely with that of clean sand as can be seen in Figure 3.

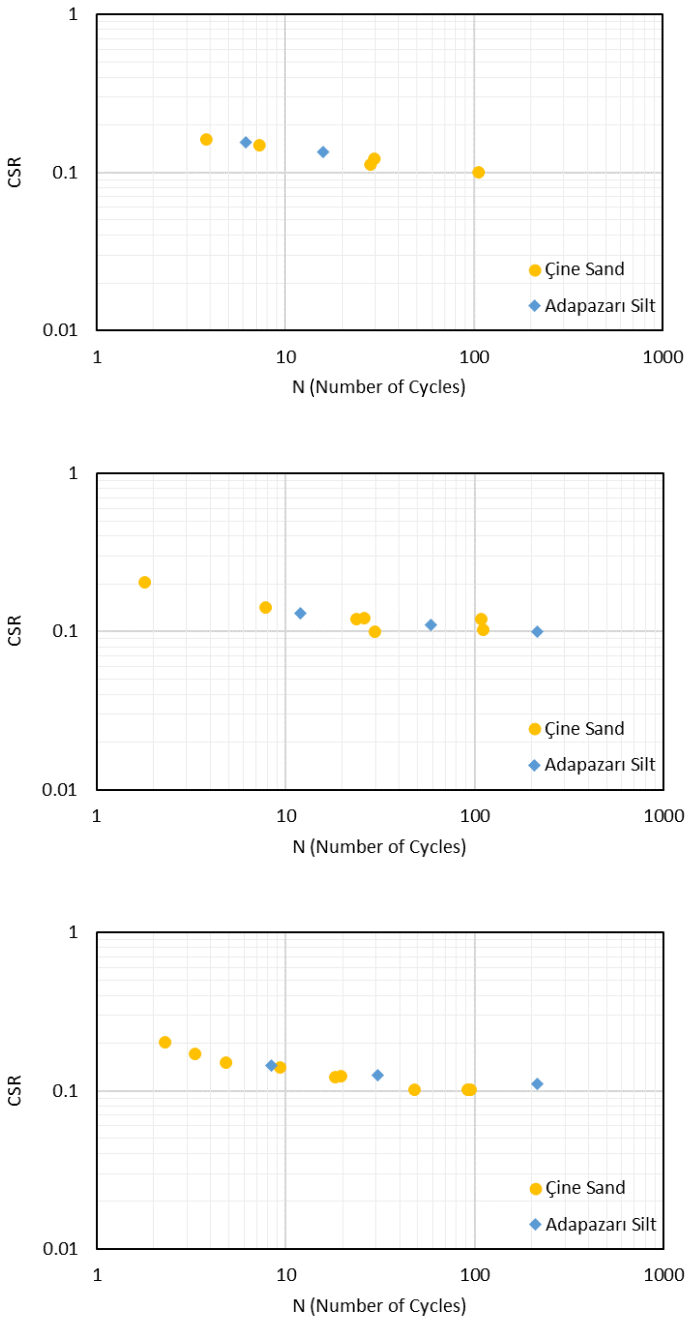

(a) $\sigma'_{v,0}$ = 50 kPa

(b) $\sigma'_{v,0}$ = 100 kPa

(c) $\sigma'_{v,0}$ = 200 kPa

Figure 3. Comparison of cyclic resistance curves for medium dense Çine sand and Adapazarı silt under initial vertical effective stress states of: (a) 50 kPa, (b) 100 kPa, and (c) 200 kPa

Furthermore, both soil types demonstrate a clear overburden stress dependence (K_σ effect) as illustrated in Figure 3. As $\sigma'_{v,0}$ increases from 50 to 200 kPa, the CSR required to reach γ_{DA} = 5% at a given cycle count systematically decreases. This proves that medium dense non-plastic silts undergo stress-dependent cyclic softening mechanisms like clean sands.

3.3. Cyclic Resistance at Dense State

At dense packing states, a distinct separation between the cyclic resistance curves of the two dry soils becomes apparent. The comparative $CSR - N_{\gamma DA=5\%}$ relationships under these initial vertical effective stress levels are shown in Figure 4a, 4b, and 4c, respectively.

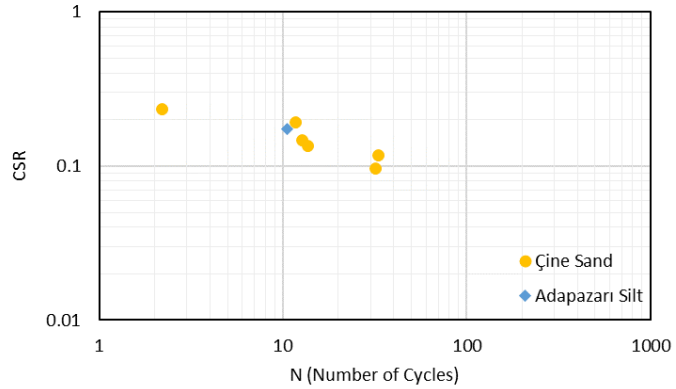

(a) $\sigma'_{v,0}$ = 50 kPa

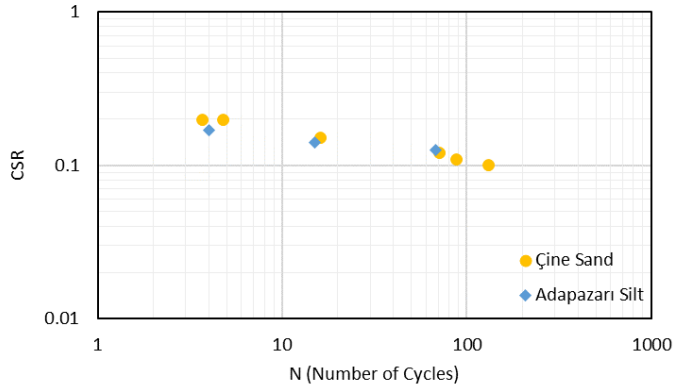

(b) $\sigma'_{v,0}$ = 100 kPa

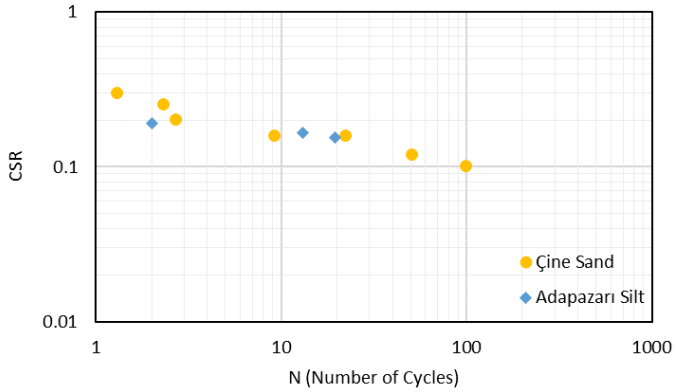

(c) $\sigma'_{v,0}$ = 200 kPa

Figure 4. Comparison of cyclic resistance curves for dense Çine sand and Adapazarı silt under initial vertical effective stress states of: (a) 50 kPa, (b) 100 kPa, and (c) 200 kPa

Unlike the loose and medium dense states where strength envelopes overlapped, the test results in Figure 4 reveal that clean Çine sand at D_r = 80% exhibits superior cyclic shear resistance compared to Adapazarı silt at D_r = 77.1%, particularly under higher confining stresses (100 and 200 kPa as shown in Figures 4b and 4c). This divergence is driven by the pronounced dilatancy tendency of dense quartz sand grains during constant-volume cyclic shearing, which temporarily maintains higher vertical effective stress levels and suppresses rapid shear strain accumulation.

Although dense Adapazarı silt also shows enhanced cyclic resistance relative to its looser states, its fine-grained matrix cannot mobilize the same magnitude of mechanical dilatant volume change tendency as dense clean sand. Consequently, for a given CSR, dense Adapazarı silt reaches the failure threshold (γ_{DA} = 5%) in fewer loading cycles (N) than dense Çine sand, aligning with classical soil mechanics expectations.

4. CONCLUSIONS

In this study, a comprehensive series of constant-volume cyclic direct simple shear (CDSS) tests was performed on dry specimens to investigate the influence of non-plastic fines on cyclic resistance by comparing clean Çine sand (SP) and pure non-plastic Adapazarı silt (ML). Tests were executed across three relative density states ($D_r \approx$ 25% - 27.9%, 41.6 - 43.8%, and 77.1 - 80%) under initial vertical effective stresses of 50, 100, and 200 kPa. Under constant-volume testing conditions, the measured loss of vertical effective stress ($\Delta\sigma'_{v,0}$) directly represents equivalent pore pressure generation (r_u).

Regarding the response at loose states, dry clean sand and non-plastic silt exhibit nearly identical $CSR - N_{\gamma DA=5\%}$ resistance curves across all tested effective overburden stresses (50 - 200 kPa). At very low relative densities, the severe contractive volume change tendency of loose sand dominates its cyclic response, resulting in a cyclic strength capacity equivalent to that of pure non-plastic silt.

Similarly, at intermediate packing states, pure non-plastic silt demonstrates a cyclic resistance capacity equivalent to that of clean sand. Within this relative density range, the non-plastic silt particles form a stable intergranular matrix capable of maintaining effective stress levels and suppressing rapid strain accumulation at a rate comparable to that of a clean sand matrix at equivalent relative densities.

Conversely, at high relative densities, a noticeable divergence in cyclic resistance occurs. Clean Çine sand exhibits higher cyclic strength than Adapazarı silt, particularly under 100 and 200 kPa initial vertical effective stresses. This behavior is attributed to the dominant dilatancy tendency and particle locking in dense sand, which fine-grained non-plastic silts cannot fully match under constant-volume conditions.

In addition to the density effects, both soil types exhibit a consistent reduction in cyclic stress ratio (CSR) capacity at failure with increasing vertical effective stress ($\sigma'_{v,0}$ = 50 to 200 kPa). This observation confirms that pure non-plastic silts are subject to overburden stress suppression (K_σ effect) mechanisms similar to those well-established for clean sands.

Contrary to conventional simplified assumptions, non-plastic silt particles—despite having significantly higher absolute void ratios—exhibit cyclic shear resistances highly comparable to those of clean sands at equivalent relative densities (Boulanger & Idriss,

2006, 2016). This indicates that grain-to-grain contact mechanisms, such as frictional sliding and skeleton stability, remain highly effective in pure non-plastic silts under constant-volume conditions (Thevanayagam et al., 2002). Overall, the findings of this study on reconstituted Çine sand and Adapazarı silt emphasize that relative density and skeletal fabric—rather than absolute void ratio or the mere presence of fine grains—serve as the primary governing controls on cyclic strength. While loose to medium dense non-plastic silts mobilize cyclic resistance equivalent to clean sands due to comparable contractive strain accumulation mechanics, dense clean sands outperform silts under higher confining stresses through enhanced dilatant behavior (Carraro et al., 2009). Consequently, liquefaction assessment frameworks should account for equivalent skeletal density and confining stress state (K_σ) rather than relying solely on generalized fines-content corrections.

REFERENCES

Aksoy, A. S. (2024). The Effects of Grain Sphericity and Roundness on Critical State Parameters (Master's thesis, Middle East Technical University).

Al-Suhaily, A. (2025). Cyclic laboratory testing-based assessment of stress scaling factors for cine sand (Doctoral dissertation, Middle East Technical University).

ASTM International. (2021). Standard test method for particle-size distribution (gradation) of fine-grained soils using the sedimentation (hydrometer) analysis (ASTM D7928-17). ASTM International.

ASTM International. (2023). Standard test methods for specific gravity of soil solids by water pycnometer (ASTM D854-14). ASTM International.

ASTM International. (2025). Standard practice for classification of soils for engineering purposes (Unified Soil Classification System) (ASTM D2487-17e1). ASTM International.

ASTM International. (2025). Standard test methods for maximum index density and unit weight of soils using a vibratory table (ASTM D4253-16e1). ASTM International.

ASTM International. (2025). Standard test methods for minimum index density and unit weight of soils and calculation of relative density (ASTM D4254-16). ASTM International.

ASTM International. (2025). Standard test methods for determining the amount of material finer than 75-μm (no. 200) sieve in soils by washing (ASTM D1140-17). ASTM International.

ASTM International. (2025). Standard test methods for particle-size distribution (gradation) of soils using particle sieve analysis (ASTM D6913/D6913M-17). ASTM International.

ASTM International. (2026). Standard test methods for liquid limit, plastic limit, and plasticity index of soils (ASTM D4318-17e1). ASTM International.

Bol, E. (2003). Adapazarı zeminlerinin geoteknik özellikleri. Sakarya Üniversitesi Fen Bilimleri Enstitüsü, İnşaat Mühendisliği, Adapazarı.

Boulanger, R. W. (2003). Relating K α to relative state parameter index. Journal of geotechnical and geoenvironmental engineering, 129(8), 770-773.

Boulanger, R. W., & Idriss, I. M. (2006). Liquefaction susceptibility criteria for silts and clays. Journal of geotechnical and geoenvironmental engineering, 132(11), 1413-1426.

Boulanger, R. W., & Idriss, I. M. (2016). CPT-based liquefaction triggering procedure. Journal of Geotechnical and Geoenvironmental Engineering, 142(2), 04015065.

Carraro, J. A. H., Prezzi, M., & Salgado, R. (2009). Shear strength and stiffness of sands containing plastic or nonplastic fines. Journal of geotechnical and geoenvironmental engineering, 135(9), 1167-1178.

Cetin, K. O., Seed, R. B., Der Kiureghian, A., Tokimatsu, K., Harder Jr, L. F., Kayen, R. E., & Moss, R. E. (2004). Standard penetration test-based probabilistic and deterministic assessment of seismic soil liquefaction potential. Journal of geotechnical and geoenvironmental engineering, 130(12), 1314-1340.

Ishihara, K. (1993). Liquefaction and flow failure during earthquakes. Geotechnique, 43(3), 351-451.

Tasbasi, A. D., Zarzour, M., Al-Suhaily, A., Kocaman, K., Bol, E., Ozocak, A., Sert, S. & Cetin, K. O. (2025, October). Cyclic Response of Adapazarı Silts Under Unidirectional Cyclic Direct Simple Shear Loading. In Turkish Conference on Earthquake Engineering (pp. 307-319). Cham: Springer Nature Switzerland.

Thevanayagam, S., Shenthan, T., Mohan, S., & Liang, J. (2002). Undrained fragility of clean sands, silty sands, and sandy silts. Journal of geotechnical and geoenvironmental engineering, 128(10), 849-859.

SYMBOL LIST

Symbol	Explanation	Symbol	Explanation
r_u	Excess pore pressure ratio	FC	Fines content
CSR	Cyclic stress ratio	PI	Plasticity index
N	Number of loading cycles	SP	Poorly graded sand
$\sigma'_{v,0}$	Initial vertical effective stress	c_u	Coefficient of uniformity
e_c or e_f	Pre-shear void ratio	c_c	Coefficient of curvature
γ_{DA}	Double amplitude shear strain	G_s	Specific gravity of soil solids
M_w	Moment magnitude	e_{max}	Maximum void ratio
ML	Low plasticity / non-plastic silt	e_{min}	Minimum void ratio
σ'_v	Vertical effective stress	NP	Non-plastic
R	Particle roundness	K_0	Coefficient of earth pressure at rest
S	Particle sphericity	e_0	Initial void ratio
$N_{\gamma DA=5\%}$	Number of cycles to reach 5% double amplitude shear strain	D_r	Relative density
$\Delta\sigma'_{v,0}$	Loss of vertical effective stress	ΔD_r	Relative density difference
K_σ	Overburden stress correction factor	e	Void ratio